Journal of the Iranian Chemical Society (2022) 19:3377–3385
https://doi.org/10.1007/s13738-022-02531-w

ORIGINAL PAPER

Application of electrochemical sensor based on nanosheets G-C_3N_4/CPE by square wave anodic stripping voltammetry method to measure residual amounts of toxic bentazon in water samples

Farzaneh Marahel[1] · Leila Niknam[1] · Elham Pournamdari[2] · Alireza Geramizadegan[3]

Received: 16 July 2021 / Accepted: 12 February 2022 / Published online: 1 April 2022

Abstract
The present work describes a method known as techniques for measuring toxic Bentazon, one of the most problematic pesticides polluting in water samples, and extremely harmful to humans and animals even at low concentrations using G-C_3N_4 nanosheets sensor. Here, we report the use of an electrochemical approach for analytical determination of toxic Bentazon that takes 100 s. The calibration curve was linear in the range of (0.2 to 16.0 µmol L^{-1}). The current response was linearly proportional to the Bentazon concentration with a $R^2 \sim 0.99$. We demonstrated a sensitivity a limits of detection of (0.2 µmol L^{-1}), and quantification of (0.22 µmol L^{-1}), were obtained for the proposed electrochemical sensor by nanosheets G-C_3N_4/CPE with (99%) which is below the U.S. Health Advisory level. Finally, the developed nanosheets G-C_3N_4/CPE based sensor was used to detect toxic bentazon in water samples with high accuracy, and sensor nanosheets G-C_3N_4/CPE were introduced for other toxics analysis in samples.

Keywords Bentazon (BTZN) · Electrochemical · Nanosheets G-C_3N_4/CPE · Voltammetric method

Introduction

Herbicides are classes of agricultural pesticides for products that improve in quality [1]. Toxic bentazon is the common name for the herbicide 3-isopropyl-1H-2,1,3-benzothiadiazin-4-(3H)-one 2, 2-dioxide and usually used to protect a crop and increase the agriculture yields [2, 3] assuming that they will be applied according to authorized agricultural patterns of good agricultural practices [3, 4]. On the other hand, the misuse of pesticides may lead to extensive concentrations of residue pesticides in the agricultural products and waters [5]. Since toxic bentazon is the widely applied herbicide, monitoring and determination of bentazon in ground and surface waters and in cultivated areas where it is used are of high significance [6]. Until now, different methods such as gas chromatography [7], liquid mass chromatography [8], liquid chromatography [9, 10]. Despite the selectivity and specificity of some analytical techniques, they are too expensive, complex, cumbersome, and time-consuming and require a larger amount of samples. On the other hand, electrochemical (SWASV) techniques have many benefits in comparison to the others, for example, simplicity, low-cost, accurateness, sensitivity, ability to determine, and electrode surface can be a good candidate in solving electrode poisoning problems [11–13].

One of the most nano-materials in recent years has been graphenes, which has attracted increasing attention as a transducer combined with biological sensing element for highly selective and sensitive, real-time response [14, 15]. lity, high-specific surface area, chemical stability, excellent catalytic activity and conductivity. These merits have made graphene an attractive channel material, also as sensing

✉ Farzaneh Marahel
Farzane.marahel.fm@gmail.com

Leila Niknam
Leila.niknam352@gmail.com

Elham Pournamdari
elhampurnamdari@gmail.com; epournamdar@iiau.ac.ir

Alireza Geramizadegan
geramialireza42@gmail.com

[1] Department of Chemistry, Omidiyeh Branch, Islamic Azad University, Omidiyeh, Iran

[2] Department of Science, Islamshahr Branch, Islamic Azad University, Islamshahr, Iran

[3] Department of Chemistry, Dashtestan Branch, Islamic Azad University, Dashtestan, Iran

element for the detection of various analytes and their characterization has become a pivotal research area in materials science research [16–18]. Graphene not only has excellent electron mobility, thermal conductivity, mechanical strength, and large surface-to-volume ratio, but also shows unique tunable ambipolar characteristics and extremely low thermal and electrical noise due to high conductivity and few surface defects [19, 20]. Accordingly, G-C_3N_4 nanosheets have very interesting features among these methods have the electrochemical (SWASV) can techniques measurement in determining BTZN be highlighted [21, 22].

This research was applied by using G-C_3N_4 nanosheets and preparing modified CPE successfully utilized for the fabrication of sensitive and specific sensors toward BTZN activity. As toxic BTZN oxidation is a two-electron transfer process, the electrochemical oxidation of toxic BTZN on nanosheets G-C3N4/CPE takes place by direct transfer of two protons and two electrons by a chemical conversion. As shown in Fig. 1, this led to the formation of nanosheets G-C_3N_4-BTZN assembly, and Fig. 2 shows the aggregated structure of G-C_3N_4 nanosheets of BTZN when they react. The sensitivity of the G-C_3N_4 nanosheets was significantly enhanced owing to the high absorbing efficiency of G-C_3N_4 nanosheets to BTZN [6, 23]. Under optimum conditions, the G-C_3N_4/CPE showed high activity to electro-oxidation of BTZN. The G-C_3N_4/CPE was

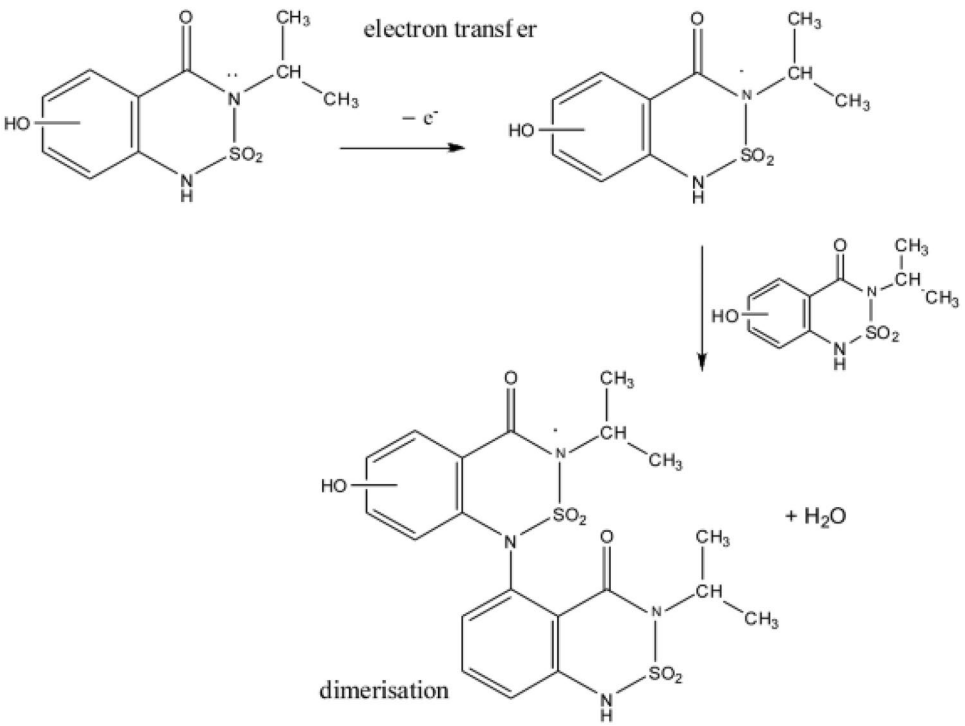

Fig. 1 The suggested mechanism of oxidation of bentazon

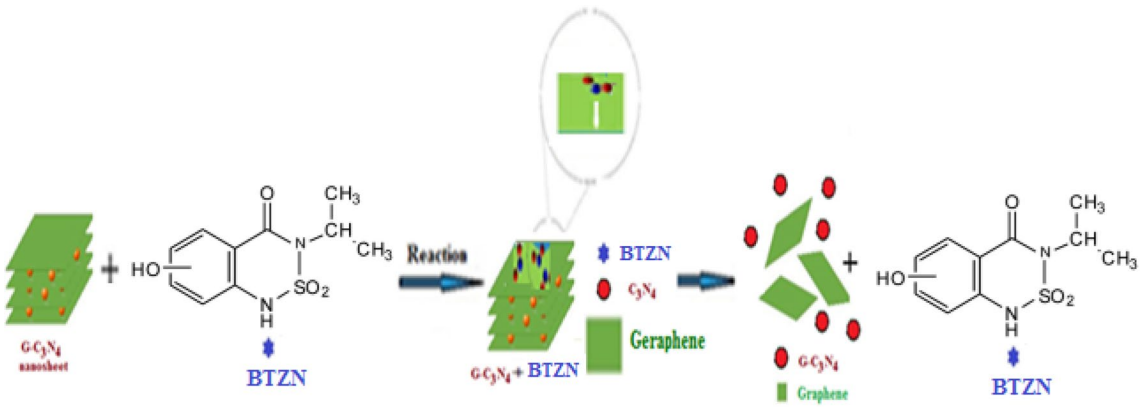

Fig. 2 Schematic of the reaction between G-C_3N_4 nanosheets and BTZN yielding G-C_3N_4 nanosheets-BTZN complex as the product

used for determination of trace amounts of BTZN on different samples.

Experimental

Materials and instrumentation

Graphite powder (10 µm average particle size) and pure paraffin oil were purchased from Merck. A stock solution of 1000 mg/L of analytical grade toxic bentazon (BTZN) (97%) from Sigma-Aldrich was prepared by dissolving 0.1 g of the BTZN in solution and diluting it to 100 mL in a volumetric flask. Absorption studies were carried out using a UV–Vis spectrophotometer model Maya Pro 180 (Shimadzu Company, Japan). For experiments, Potentiostat/galvanostat system (Model SAMA 500 Esfahan, Iran) and a copper wire, an Ag/AgCl/KCl (3 $molL^{-1}$) were used. Transmission Electron Microscopy (TEM) images (Zeiss EM902A), X-ray diffractometer (38,066 Riva, d/G. Via M. Misone, 11/D (TN)). The pH was measured using an Inolab wtw720 (Germany).

Sample preparation

Water samples were collected from Karkheh dam water, Dez dam water, and Karun River, Iran. All the water samples were filtered using 0.45 µm micropore membranes to remove suspended particles and the pH water samples were adjusted to 3.5 followed by storing in glass containers at 4 °C [24].

Procedure synthesis sensor G-C_3N_4 nanosheets

To synthesis the G-C_3N_4, one gram of melamine was placed on a ceramic quartz boat crucible and heated at a rate of 5 °C min to 550 °C in a furnace for 3 h. The crucible was then cooled to room temperature, and the light-yellow colored G-C_3N_4 was collected, as shown in Fig. 3 [25, 26]. It is worth mentioning that as-synthesized bulk G-C_3N_4 has poor conductivity, poor water solubility, and large particle size (low specific area), so it is not suitable for electrochemical applications. The exfoliated ultrathin G-C_3N_4 nanosheets have higher specific surface area and provide more surface-active sites. More importantly, reports have demonstrated that the ultrathin G-C_3N_4 nanosheets activity and stability than bulk G-C_3N_4 nanosheets have better electrochemical; this suggests that exfoliated ultrathin G-C_3N_4 nanosheets are a promising candidate material for electrochemical applications [27]. The bare CPE adopted an aqueous phase exfoliation method for the preparation of G-C_3N_4 nanosheets. Herein, 0.05 g G-C_3N_4 was stirred for 1 h and then ultrasonicated in a hot water bath. Once the reaction is completed, it cools naturally to ambient temperature until a clear solution was persed containing G-C_3N_4 nanosheets [23, 28].

Analytical procedure

The analyte of toxic BTZN by SWASV technique was performed in an electrolytic cell having Platinum thin wire as counter, Ag/AgCl, as a reference, whereas either pare GCE

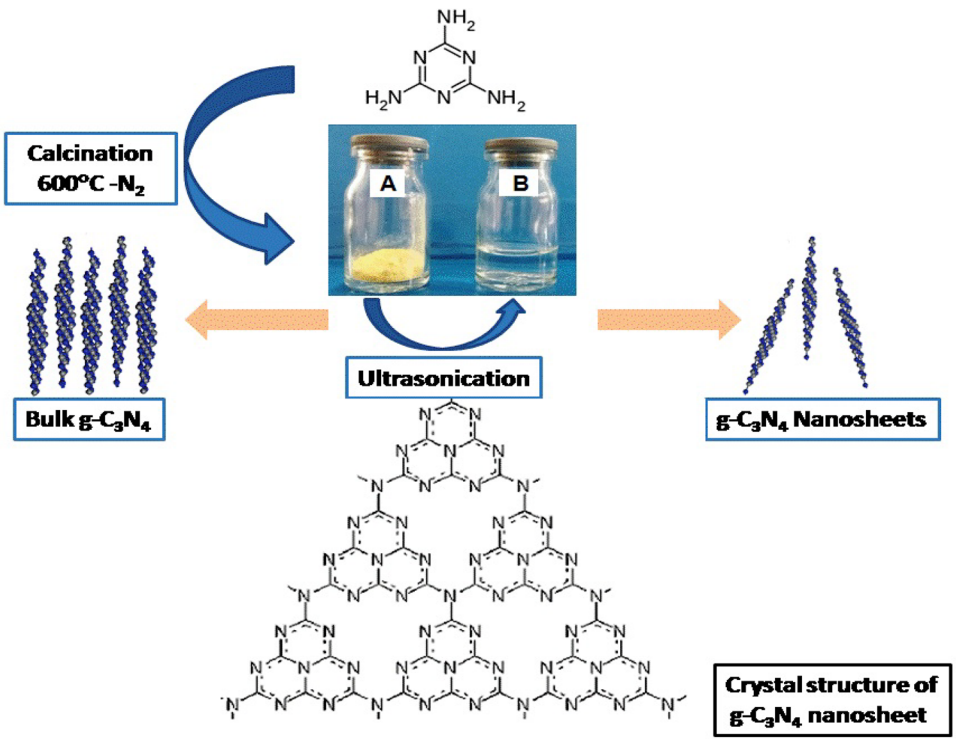

Fig. 3 **A** Schematic of G-C_3N_4 nanosheet synthesis **B** obtained after G-C_3N_4 ultrasonic treatment

or Ag/AgCl-nanosheets G-C_3N_4 was used as working electrode in 20 mL capacity cell, and 1 ml of 0.1 M acetate buffer as a supporting electrolyte medium investigated, pH of the solution under all optimized parameters was 3.5. The solution of BTZN was investigated at a potential range, − 0.6 to 0.4 V, and peak currents were measured at potentials of about 0.2 V vs. Ag/AgCl for BTZN, 100 s, respectively [28].

Results and discussion

Characterization of synthesized G-C_3N_4 nanosheets

Figure 4 shows the SEM, TEM morphology and particle diameter result G-C_3N_4 nanosheets. The surface morphology G-C_3N_4 nanosheets are recorded by the SEM as shown in Fig. 4a, b, which revealed the presence of agglomerated particles. The G-C_3N_4 nanosheet shapes are distorted spherical, with an average size range of 25–30 nm as shown by SEM image (Fig. 4a, b) and shown by TEM image in Fig. 4c. Upon the addition of BTZN, G-C_3N_4 nanosheets aggregated due to the presence of substance with groups S and N [23, 25]. Different X-ray emission peaks are G-C_3N_4 nanosheets shown in Fig. 4d. The signal at $2\theta = 28.5°$ is ascribable to diffractions and reflections from the carbon atoms. The positions of diffraction peaks are in agreement with the standard samples of G-C_3N_4 nanosheets [27, 28].

Electrochemical oxidation of toxic BTZN by nanosheets G-C_3N_4/CPE

Electrochemical oxidation of 10.0 µmol L^{-1} of toxic BTZN was tested on a bare CPE and nanosheets G-C_3N_4/CPE (at a scan rate of 50 mV s^{-1} in nanosheets G-C_3N_4/CPE is illustrated in Fig. 5. The impact of scan rate (υ) on toxic BTZN oxidation peak current (I_P) was investigated at G-C_3N_4 using an electrochemical (SWASV) measurement method. In the Randles–Sevcik formula (Eq. 1), it can be clearly seen that

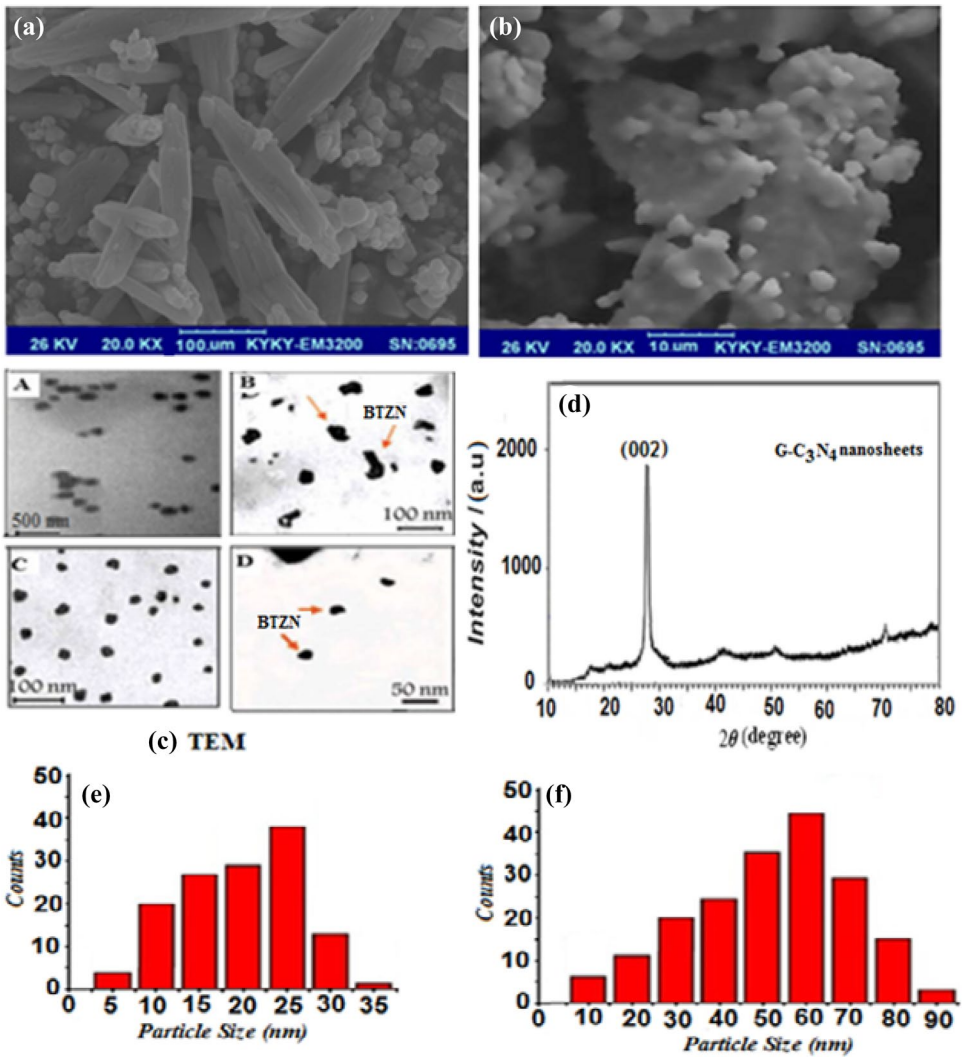

Fig. 4 The **a** SEM image of the G-C_3N_4 nanosheets in 100 nm. The **b** SEM image of the prepared G-C_3N_4 nanosheets in 10 nm. **c** TEM image of G-C_3N_4 nanosheets before and after addition of toxic BTZN analysis. G-C_3N_4 nanosheets (**A**) G-C_3N_4 nanosheets-BTZN (**B**) Close-up image of G-C_3N_4 nanosheets (**C**) Close-up image of G-C_3N_4 nanosheets-BTZN (**D**). **d** XRD pattern of synthesized G-C_3N_4 nanosheets. **e** Size analysis of G-C_3N_4 nanosheets (**f**) G-C_3N_4 nanosheets – BTZN

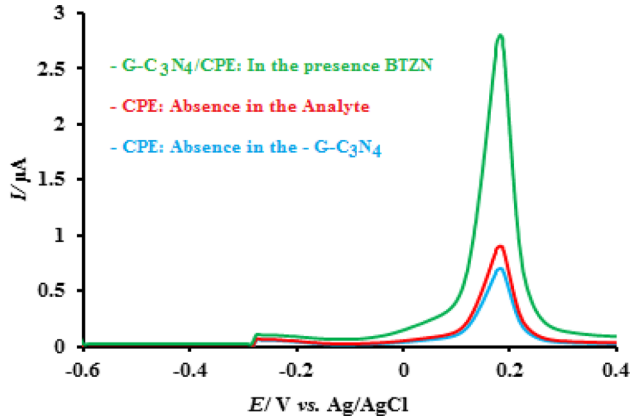

Fig. 5 SW voltammograms in the absence electrolyte and presence 10.0 µmol L^{-1} of BTZN in electrochemical conditions on the surface of bare CPE: (line green) absence by G-C_3N_4 in the presence BTZN, (line red) absence CPE of the analyte and (line blue) absence G-C_3N_4 nanosheets/CPE

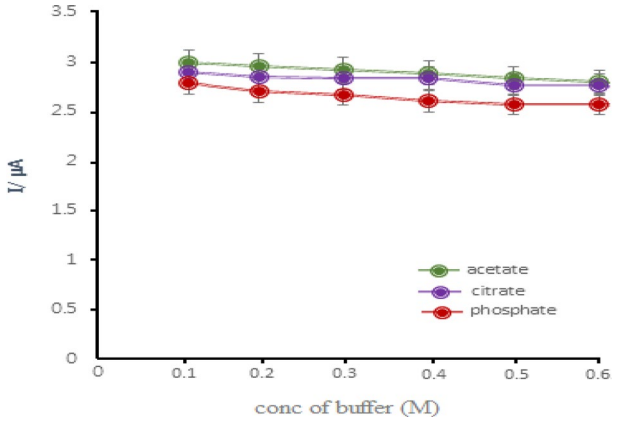

Fig. 6 Effect of buffer on the voltammetric current for 10.0 µmol L^{-1}, toxic BTZN solution

the increases against square roots of scan rate with a linear correlation coefficient of (R^2 pa Where Ip) 0.9992 (Fig. 8b) [29].

$$Ip = \left(2.69 \times 10^5\right) n^{3/2} A D^{1/2} C v^{1/2} \quad (1)$$

The oxidation peak current (A), n is the number of transferred electrons per mole, A is the active surface area of the electrode (cm^2), D is the diffusion coefficient (cm^2/sec), C is the concentration (mol/cm^3) and ν is the scan rate (V/s) [30].

SW voltammograms in the absence of electrolyte and presence of toxic BTZN in electrochemical conditions

To realize individual detection of BTZN by electrochemical SWV measurement method, at first, the working electrode has been modified with a modified material by putting it into a mixture solution including in acetate buffer (pH 3.5) and BTZN. In order to obtain well-defined (SWASV) peaks and the best response, the electrochemical measurements from − 0.6 to 0.4 V; the amplitude 0.2 V; the step height potential 6 mV; the time of integration 10 s; and the frequency 50 Hz were done. As shown in Fig. 5, potential 0.2 V vs and nanosheets G-C_3N_4/CPE can be useful for the determination of BTZN in an aqueous solution [23, 31]. After adding each analyte, distinct stripping peaks can be seen for toxic BTZN in the peak separation of 0.2 V *vs*. Ag/AgCl. This peak was attributed to facilitating electron transfer between toxic BTZN and nanosheets G-C_3N_4/CPE. The response of modified electrode is dependent on many factors including pH of the solution, accommodation potential, time, and the instrumental parameters of SWV in the lowest detection limit. Based on these observations, it is convenient, nanosheets G-C_3N_4/CPE can be useful for determination of toxic BTZN in aqueous solution [11, 32].

Optimization of sensing conditions

In order to reach the best result response in detecting BTZN rests upon the systematic optimization of pH, buffer, and incubation time step by step were optimized.

Impact of buffer

In this section, the best type of buffer (citrate, acetate and phosphate buffer), and its volume for a maximum of BTZN availability for detection purposes with nanosheets G-C_3N_4/CPE sensor are investigated. Furthermore, 1.0 mL of acetate buffer was selected as optimum. It can clearly be seen from Fig. 6 [23].

Impact of pH

According to data, pH 3.5 produced the best results as compared to other pH values among the pH range from 2 to 7. Thus, this pH could be useful for stability of deposited nanosheets G-C_3N_4/CPE at electrode. As shown in Fig. 7a, the peak current was decreased by further increasing pH; it may be owing to the BTZN hydrolysis. Hence, the pH of 3.5 was selected for the subsequent experiment [33, 34].

Impact of deposition time

The impact of deposition time on the stripping responses of BTZN was studied from 25 to 150 s with a deposition potential of 0.2 V, and it has been found that the oxidation response is increased by increasing accumulation time up to

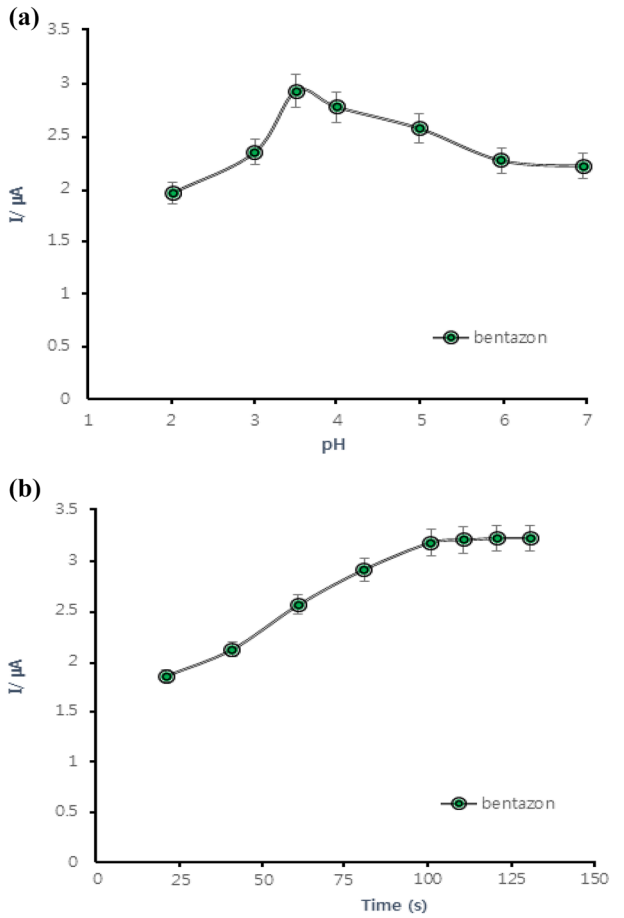

Fig. 7 **a** Effect of pH on the voltammetric currents for 10.0 µmol L^{-1} of BTZN solution. **b** Effect of deposition time on the voltammetric currents for 10.0 µmol L^{-1} of BTZN solution

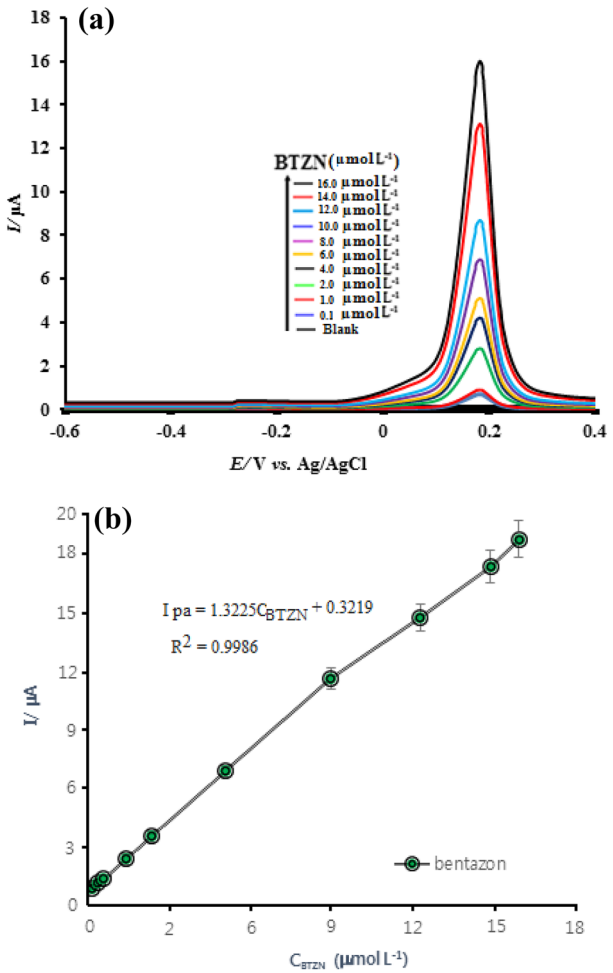

Fig. 8 The modified electrode G-C_3N_4 nanosheets/CPE in the analyte BTZN. (a) SW Voltammograms using C_{BTZN} the analytes, (b) BTZN Calibration curve diagram (0.1–16.0 µmol L^{-1}) solution, pH 3.5, time 100 s, in acetate buffer

100 s [34]. Therefore, the accumulation time, a reaction time of 100 s, was chosen in this experiment as shown in Fig. 7b.

Analytical application

This section purposes the examined and analytical performance of G-C_3N_4 nanosheets/CPE for the determination of BTZN. First, examined and drawn voltammogram, solution with different concentrations of BTZN from (0.2 to 16.0 µmol L^{-1}) using the (SWASV) technique, which is shown in Fig. 8a. Also, in the BTZN calibration equation, shown in Fig. 8b, it can be seen there is a direct and linear relationship between the concentration and the peak oxidation current, and peak oxidation current the concentration of BTZN gradually increases. Also, for 10 replicate measurements of 0.2 µmol L^{-1} BTZN solution under optimized conditions, the relative standard deviation was (2.2%), limits of detection (LOD) of (0.2 µmol L^{-1}), and quantification (LOQ) of (0.22 µmol L^{-1}), respectively (Fig. 8b) [11, 23].

Evaluation of reproducibility and stability of the modified electrode

G-C_3N_4 nanosheets/CPE electrode reproducibility by recording SW Voltammetry repeated n (10) from constant concentrations 10.0 µmol L^{-1} of BTZN, pH 3.5 and extracting peak currents from each voltammogram studied the relative standard deviation (RSD) was (± 2.2%), and detection of the method (0.2 µmol L^{-1}) for (BTZN), which indicates the excellent reproducibility and the high accuracy of the introduced analytical method. Then, the impact of electrode shelf life and stability was compared after one month and two months by comparing the voltammogram results with the initial voltammogram results. The obtained currents had reached 94.2% and 94.4% of their initial values, respectively. Also, the response of electrodes for 10.0 µmol L^{-1} of BTZN-G-C_3N_4 nanosheets retained 94.0% of its initial stripping response after a period of two months. The results indicate

that the G-C_3N_4 nanosheets/CPE has excellent repeatability, reproducibility, and long-term stability [24, 35].

Studies detection electrochemical behavior of simultaneous bentazon (BTZN) and other herbicides at the nanosheets G-C_3N_4/CPE

It is essential to develop a fast and user-friendly sensor for determining problematic pesticides with low cost, high sensitivity, and selectivity. The simultaneous detection of the analytes is depicted in Fig. 9, SW voltammograms (10.0 µmol L^{-1}) of the analytes in phosphate buffer (pH 3.5, 0.1 M) at the bare CPE and G-C_3N_4/CPE by for 100 s. Bentazon (BTZN) accumulation potential 0.2 V *vs.* As shown in Fig. 9, acceptable results have been obtained simultaneous detection for BTZN in the presence of other analytes [11, 23].

Investigation of competition of bentazon (BTZN) with other ions

The study was performed in the presence of cations and anions in a solution containing 10.0 µmol L^{-1} of BTZN in pH 3.5, and acetate buffer (0.1 M), the bare CPE, and G-C_3N_4/CPE by for 100 s in the potential (0.2 V *vs*). Ag/AgCl. The results are shown in Fig. 10 [23, 36].

Recovery evaluation for real samples

Sensor testing performance of the developed using the modified G-C_3N_4 nanosheets/CPE electrode was successfully used to measure toxic BTZN in water samples and the results were compared by standard spectrophotometric methods, and the total amount of the measure toxic BTZN was estimated ($n = 3$). The results are summarized in Table. 1. Firstly, analysis of the samples provided the absence of the toxic BTZN and then the accuracy of the mentioned method was evaluated by analyzing the samples spiked with the known amount of the toxic BTZN. Satisfactory spiked recovery results illustrated that the matrix effects were unimportant for determining the toxic BTZN in some natural real samples (Table. 1) [36]. By comparing the results of toxic BTZN measurements with the proposed method and standard spectrophotometric methods and evaluating them with a t-Test, it was found that there is no significant difference. These results characterized that the new method for determining toxic BTZN is appropriate for the quality control and determination of toxic BTZN in water samples [37, 38].

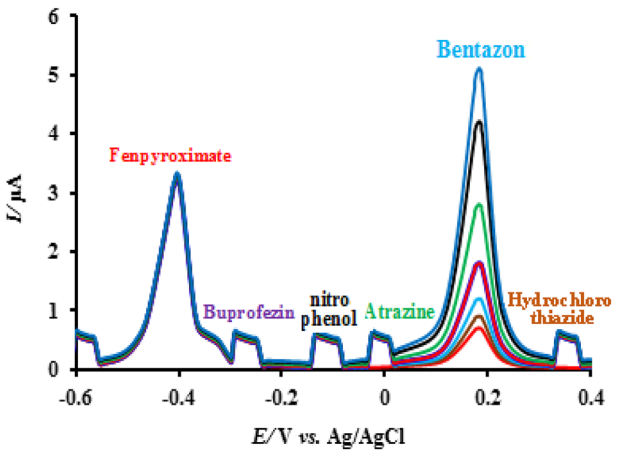

Fig. 9 The modified electrode G-C_3N_4 nanosheets/CPE in the analyte solutions of simultaneous detection of the analyte bentazon (BTZN), and other herbicides (10 µmol L^{-1}) solution, pH 3.5, time 100 s, in acetate buffer

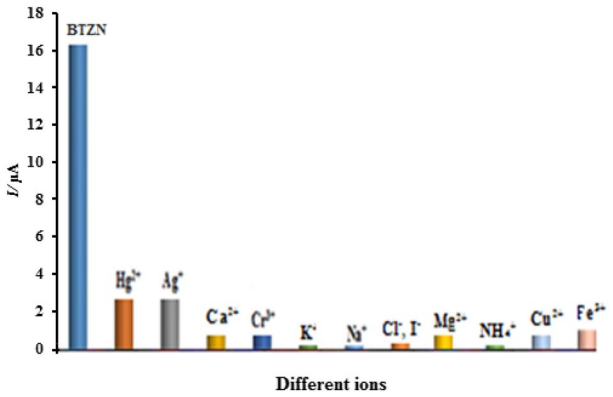

Fig. 10 Impacts of the different ions on the determination of the bentazon (BTZN) with G-C_3N_4 nanosheets/CPE (pH 3.5, time 100 s, in acetate buffer

Comparison of presented work with other electrodes for the measurement of toxic BTZN

The proposed electrochemical sensor could be renewed quickly and easily by mechanical polishing whenever needed. Comparisons of different electrodes for the determination of toxic BTZN are shown in Table 2. The proposed sensor shows good selectivity, reproducibility, repeatability, and stability.

Conclusions

This study describes a method (SWASV) for the determination of toxic BTZN one of the most problematic pesticides polluting in water samples, and extremely harmful to humans and animals even at low concentrations using G-C_3N_4 nanosheets sensor. Applying provides a modified carbon paste electrode based on G-C_3N_4 nanosheets for the determination of toxic BTZN in Karun River water, Karkheh

Table 1 Detection of amounts of residual toxic BTZN in water samples ($n=3$)

Samples	Added (μmol mL^{-1})	Founded by SWV (μmol mL^{-1})	Founded by UV.vis spectrophotometer (μmol mL^{-1})	t_{exp}	Recovery %
Karun river water Ahvaz	0	2.8 ± 2.7	2.7 ± 2.5	0.92	—
	5	7.7 ± 1.6			97.6
	10	12.7 ± 1.5			99
Dez dam water	0	3.6 ± 1.8	3.8 ± 1.8	2.33	—
	5	8.7 ± 1.0			102
	10	13.6 ± 1.4			102
Karkheh dam water	0	2.9 ± 2.7	3.0 ± 2.8	0.97	—
	5	8.0 ± 1.8			98
	10	12.9 ± 1.6			97.7

Mean value ± standard deviation, ($n=3$)

The recovery was calculated on the basis of the obtained results from the Square Wave Anodic Stripping Voltammetry (SWASV) Method

Table 2 Comparison of Linear range and DL of the some recently suggested electrodes for the determination of BTZN

Analyte	Modified electrode/method	Linear range (μmol L^{-1})	D L (μmol L^{-1})	References
Bentazon (BTZN)	boron-doped diamond electrode(BDD)/ CPE (SWV)	9.9–91.0	4.95	[11]
Bentazon (BTZN)	Poly-Ac MnODEAETPc/GCE (SWV)	50–750.0	0.25	[12]
Bentazon (BTZN)	BDDE (DPV)	2.0–100.0	0.5	[14]
Bentazon (BTZN)	SPE//GCE (SWV)	0.19–50.0	0.034	[24]
Bentazon (BTZN)	Carbon Nanotube ß Cyclodextrin (CV)	10.0–80.0	1.6	[31]
Bentazon (BTZN)	G-C_3N_4/CPE (SWV)	0.2 -16.0	0.2	This work

dam water, and Dez dam water. The calibration curve was linear in the range of (0.2–16.0 μmol L^{-1}). The standard deviation method (0.2 μmol L^{-1}) and quantification (LOQ) of (0.022 μmol L^{-1}) for toxic BTZN were obtained for the proposed electrochemical sensor by G-C_3N_4 nanosheets, respectively. The application of the sensor in the natural water sample and its validation with the standard addition method for toxic BTZN detection confirms its authenticity for application in nearly every type of water. Moreover, the developed sensor holds promises for implementation in a wide range of environments including biological and water samples.

Acknowledgements We gratefully thank Islamic Azad University Omidiyeh Branch, Omidiyeh, Iran, for financial support.

Conflict of interest No potential conflict of interest was reported by the author(s).

References

1. H.M. Salman, B.H. Hameed, Effect of preparation conditions of oil palm fronds activated carbon on adsorption of bentazon from aqueous solutions. J. Hazard. Mater. **175**, 133 (2010)
2. N.A. Mir, M.M. Haque, A. Khan, M. Muneer, S. Vijayalakshmi, Photocatalytic degradation of herbicide Bentazone in aqueous suspension of TiO_2: mineralization, identification of intermediates and reaction pathways. Environ. Technol. **35**, 407 (2014)
3. A. Schuhmann, G. Klammler, S. Weiss, O. Gans, J. Fank, G. Haberhauer, M.H. Gerzabek, Degradation and leaching of bentazone, terbuthylazine and S-metolachlor and some of their metabolites: A long-term lysimeter experiment. Plant. Soil. Environ. **65**, 273 (2019)
4. M.C. Bruzzoniti, R.M. De Carlo, L. Rivoira, M. Del Bubba, M. Pavani, M. Riatti, B. Onida, Adsorption of bentazon herbicide onto mesoporous silica: application to environmental water purification. Environ. Sci. Pollut. Res. **23**, 5399 (2016)
5. M.J. Hedegaard, H. Deliniere, C. Prasse, A. Dechesne, B.F. Smets, H.J. Albrechtsen, Evidence of co-metabolic bentazone transformation by methanotrophic enrichment from a groundwater-fed rapid sand filter. J. Water Res. **129**, 105 (2018)
6. F. Marahel, L. Niknam, Enhanced fluorescent sensing probe via PbS quantum dots functionalized with gelatin for sensitive determination of toxic bentazon in water samples. Drug Chem. Toxicol. **44**(4), 1–9 (2021). https://doi.org/10.1080/01480545.2021.1963761
7. H. Guan, W.E. Brewer, S.T. Garris, S.L. Morgan, Disposable pipette extraction for the analysis of pesticides in fruit and vegetables using gas chromatography/mass spectrometry. J. Chromatogr. A. **1217**, 1867 (2010)
8. B. Cho, S. Kim, S. In, S. Choe, Simultaneous determination of bentazon and its metabolites in postmortem whole blood using

liquid chromatography-tandem mass spectrometry. Forensic Sci. Int. **278**, 304 (2017)
9. S.S. Takla, F.M.S.E. El-Dars, A.S. Amien, M.A. Rizk, Analysis of fenpyroximate residues in eggplant, aubergine (Solanum melongena L.) during crop production cycle by HPLC and determination of its biological activity. Egypt. Acad. J. Biolog. Sci. **12**(1), 163 (2020)
10. P. Norouzi, B. Larijani, F. Faridbod, M.R. Ganjali, Anovel method for ultra trace measurement of Bentazon based on nanocomposite electrode and continuous coulometric FFT cyclic voltammetry. Int. J. Environ. Res. **9**, 101 (2015)
11. L. Codognoto, T.S. Lima, F.R. Simoes, H.D.T. Da Silva, E.M.A. Valle, D-optimal design for electrochemical simultaneous determination of bentazon and fenamiphos in natural waters. Int. J. Environ. Anal. Chem. **101**(14), 1–17 (2021). https://doi.org/10.1080/03067319.2021.2007241
12. L.A. Akinbulu, T. Nyokong, Characterization of polymeric film of a new manganese phthalocyanine complex octa-substituted with 2-diethylaminoethanethiol, and its use for the electrochemical detection of bentazon. Electrochim. Acta. **55**, 37 (2009)
13. A. Khanmohammadi, A. Jalili Ghazizadeh, P. Hashemi, A. Afkhami, F. Arduini, H. Bagheri, An overview to electrochemical biosensors and sensors for the detection of environmental contaminants. J. Iran. Chem. Soc. **17**(10), 2429 (2020). https://doi.org/10.1007/s13738-020-01940-z
14. S. Jevtic, A. Stefanovic, D.M. Stankovic, M.V. Pergal, A.T. Ivanovic, A. Jokic, B. Petkovic, Boron-doped diamond electrode — a prestigious unmodified carbon electrode for simple and fast determination of bentazon in river water samples. Diam. Relat. Mater. **81**, 133 (2018)
15. J. Shu, D. Tang, Recent advances in photoelectrochemical sensing: from engineered photoactive materials to sensing devices and detection modes. Anal. Chem. **92**(1), 363 (2020)
16. H. Beitollahi, S.Z. Mohammadi, M. Safaei, S. Tajik, Applications of electrochemical sensors and biosensors based on modified screen-printed electrodes: a review. Anal. Methods. **12**, 1547 (2020)
17. Y. Qin, Y. Liu, Y. Kong, F. Chu, Electrochemically exfoliating graphite into N-doped graphene and its use as a high efficient electrocatalyst for oxygen reduction reaction. J. Solid. State. Electrochemistry. **21**(5), 1287 (2017)
18. K. Zhang, S. Lv, Q. Zhou, D. Tang, CoOOH nanosheets-coated g-C_3N_4/$CuInS_2$ nanohybrids for photoelectrochemical biosensor of carcinoembryonic antigen coupling hybridization chain reaction with etching reaction. Sens. Actuators. B. **307**, 127631 (2020)
19. J.S. Noori, J. Mortensen, A. Geto, Rapid and sensitive quantification of the pesticide lindane by polymer modified electrochemical sensor. Sensors. **21**(2), 393 (2021)
20. M.A. Karimi, V.H. Aghaei, A. Nezhadali, N. Ajami, Graphitic carbon nitride as a new sensitive material for electrochemical determination of trace amounts of tartrazine in food samples Food Anal. Methods. **11**(10), 2907 (2018). https://doi.org/10.1007/s12161-018-1264-4
21. A.M. Babu, R. Rajeev, D.A. Thadathil, Surface modulation and structural engineering of graphitic carbon nitride for electrochemical sensing applications. J. Nanostruct. Chem. **11**(4), 1–14 (2021). https://doi.org/10.1007/s40097-021-00459-w
22. J. Hong, J. Kim, R. Selvaraj, Y. Kim, Immobilization of visible-light-driven photocatalyst g-C_3N_4 ceramic fiber for degradation of organic dye. Toxicol. Environ. Chem. **103**(3), 18 (2021). https://doi.org/10.1016/j.etap.2020.103552
23. F. Marahel, G-C_3N_4 nanosheets-based sensing interface for square-wave anodic stripping voltammetric detection of 2-mercaptobenzothiazole in water samples. Int. J. Environ. Anal. Chem. **101**, 1–12 (2021). https://doi.org/10.1080/03067319.2021.1983557
24. A. Geto, J.S. Noori, J. Mortensen, W.E. Svendsen, M. Dimaki, Electrochemical determination of bentazone using simple screen-printed carbon electrodes. Environment. Int. **129**, 400 (2019)
25. A. Hatamie, F. Marahel, A. Sharifat, Green synthesis of graphitic carbon nitride nanosheet (g-C_3N_4) and using it as a label-free fluorosensor for detection of metronidazole via quenching of the fluorescence. Talanta **176**, 518 (2018)
26. Y.P. Zhu, T.Z. Ren, Z.Y. Yuan, Mesoporous phosphorus-doped g-C_3N_4 nanostructured flowers with superior photocatalytic hydrogen evolution performance. ACS. Appl. Mater. Interfaces. **7**(30), 16850 (2015)
27. N. Murugan, M.B. Chan-Park, A.K. Sundramoorthy, Electrochemical detection of uric acid on exfoliated nanosheets of graphitic-like carbon nitride (g-C) based sensor. J. Electrochem. Soc. B. **166**(9), 3163 (2019)
28. M.H. Vu, C.C. Nguyen, T.O. Do, Graphitic carbon nitride (g-C_3N_4) nanosheets as a multipurpose material for detection of amines and solar-driven hydrogen production. Chem. Photo. Chem. **5**(5), 466 (2021). https://doi.org/10.1002/cptc.202000265
29. N. Tukimin, J. Abdullah, Y. Sulaiman, Review—electrochemical detection of uric acid, dopamine and ascorbic acid. J. Electrochemical. Soc. **165**(7), B258 (2018). https://doi.org/10.1016/j.arabjc.2018.09.002
30. L. Chao, Y. Qin, Y. Liu, Electrochemically exfoliating graphite into N-doped graphene and its use as a high efficient electrocatalyst for oxygen reduction reaction. J. Solid State. Electrochem. **21**, 1287 (2017). https://doi.org/10.1007/s10008-016-3480-4
31. V. Rahemi, J.M.P.J. Garrido, F. Borges, C.M.A. Brett, E.M.P. Garrido, Electrochemical determination of the herbicide bentazone using a carbon nanotube β-cyclodextrin modified electrode. J. Electroanalysis. **25**, 2360 (2013)
32. T. Rahmani, H. Bagheri, A. Afkhami, Modified 3D graphene-au as a novel sensing layer for direct and sensitive electrochemical determination of carbaryl pesticide in fruit, vegetable, and water samples. Food Anal. Methods. **11**(11), 3005 (2018). https://doi.org/10.1007/s12161-018-1280-4
33. A. Mishra, A. Mehta, S. Basu, N.P. Shetti, K.R. Reddy, T.M. Aminabhavi, Graphitic carbon nitride (g–C_3N_4)–based metal-free photocatalysts for water splitting. A Rev Carbon. **149**(4), 693 (2019)
34. A.R. Rautio, O. Pitkanen, T. Jarvinen, A. Samikannu, N. Halonen, M. Mohl, J.P. Mikkola, K. Kordas, Single-layered mesoporous carbon sandwiched graphene nanosheets for high performance ionic liquid supercapacitors. J. Phys. Chem. C. **119**, 3538 (2015)
35. F. Hasanpour, M. Teimoury, A. Eghbali, Electroanalysis of bentazon residues in salvia officinalis extract essential oils using $ZnFe_2O_4$ anchored on reduced graphene oxide nanoparticles modified electrode. Iran. J. Anal. Chem. **5**(2), 56 (2018)
36. C. Yanez, M. Araya, S. Bollo, Complexation of herbicide bentazon with native and modified β-cyclodextrin. J. Incl. Phenom. Macrocycl. Chem. **68**, 237 (2010)
37. B. Wang, G. Ding, J. Zhu, W. Zhang, M. Guo, Q. Geng, D. Guo, Y. Cao, Development of novel ionic liquids based on bentazone. Tetrahedron **71**, 7860 (2015)
38. T. Gan, J. Sun, W. Meng, L. Song, Y. Zhang, Electrochemical Sensor based on graphene and mesoporous TiO_2 for the simultaneous determination of trace colourants in food. J. Food Chem. **141**(4), 3731 (2013)